Experimental and Theoretical Electronic Structure Investigations on α-Nb_3Cl_8 and the Intercalated Phase β′-$NaNb_3Cl_8$

John Rory Kennedy,*,† Peter Adler,* Richard Dronskowski, and Arndt Simon

Max-Planck-Institut für Festkörperforschung, Heisenbergstrasse 1, 70 569 Stuttgart, Germany

Received October 18, 1995[⊗]

The electronic structures of the cluster compound α-Nb_3Cl_8 and the intercalated phase β′-$NaNb_3Cl_8$ have been studied by core level and valence band X-ray and ultraviolet photoelectron spectroscopy (XPS and UPS), diffuse reflectance spectroscopy, and charge-self-consistent molecular orbital (CSC-EH) and band structure (CSC-EH-TB) calculations. The crystal structures of the two compounds consist of layers of interconnected Nb_3Cl_{13} units. XP and UP valence band spectra as well as the band structure calculations show well separated sets of Cl 3p levels at lower energy (higher binding energy) and Nb 4d levels at higher energy (lower binding energy), indicative of mainly ionic Nb−Cl bonding. The UP spectra of α-Nb_3Cl_8 reveal a triple-peak structure for the Nb 4d levels, corresponding to the $1a_1$, 1e, and $2a_1$ metal−metal bonding orbitals of a seven-electron Nb_3 cluster as suggested by theory. The valence band shapes are in good agreement with the theoretical density-of-states curve. The relative intensities in the XP valence band spectra of β′-$NaNb_3Cl_8$ evidence an additional electron in the Nb 4d orbitals. The better resolved UP spectra, however, show a broad pattern for the Nb 4d levels which is neither expected from a single cluster model nor given by the theoretical density-of-states curve. Possible origins for this discrepancy between experiment and theory are discussed. Electrostatic interactions between Na^+ and Cl^- ions in β′-$NaNb_3Cl_8$ lead to a narrowing of the Cl 2p core level and Cl 3p valence band signals, the former being shifted to higher binding energy in comparison to α-Nb_3Cl_8. Two rather narrow absorptions in the optical spectra of α-Nb_3Cl_8 are assigned to the transitions from the $1a_1$ and 1e levels into the singly occupied $2a_1$ orbital. These absorptions are missing in the optical spectra of β′-$NaNb_3Cl_8$, in agreement with the theoretical expectations for an eight electron Nb_3 cluster.

1. Introduction

The formation of β′-$NaNb_3Cl_8$ from an ambient temperature reaction of solid α-Nb_3Cl_8 with a solution of Na_2bzph (bzph = benzophenone) represented the first report[1] on a new subclass of intercalation compounds: binary metal halides containing local or extended metal−metal bonding. Additional compounds of this type shown to undergo this redox reaction with either Na or Li until now include Nb_3Br_8, Nb_6I_{11}, and the metal-halide−carbide $Y_2I_2C_2$.[2] In fact, the only other binary metal halides previously known to react by intercalation of the third body species (with the exception of hydrogen) were $RuCl_3$ and $RuBr_3$,[3] but these are not described with metal−metal bonding. One reason for the apparent propensity of metal−metal-bonded binary metal halides to undergo this reaction may lie in the ability of the metal−metal bonding energy levels to allow for a flexibility in their electronic stability.

The crystal structure of α-Nb_3Cl_8 can be described[4,5] as a layer structure built up from triangular Nb_3Cl_{13} units which are interconnected by bridging chlorine atoms. A preliminary structure determination of β′-$NaNb_3Cl_8$ (Rietveld method) revealed only small structural changes compared to the parent compound α-Nb_3Cl_8. The primary differences are a phase transition to another stacking variant (hcp to ccp anion lattice), a small decrease in Nb−Nb cluster bond lengths (about 4 pm), and a greater general distortion of the octahedral chloride environment around the Nb centers. On the other hand, a distinct color change occurs upon the addition of an electron to α-Nb_3Cl_8 as the parent compound is olive green and the sodium intercalated β′-$NaNb_3Cl_8$ is a rich red-violet. Group theoretical molecular orbital considerations regarding these structural type compounds reveal a pattern of metal−metal bonding and antibonding orbitals which form the highest occupied and lowest unoccupied states.[1,6]

In order to more quantitatively explore the electronic structure of the parent compound α-Nb_3Cl_8 and the changes which occur due to sodium intercalation, we have investigated the two compounds by X-ray and UV photoelectron spectroscopy, diffuse reflectance spectroscopy, and finally by charge-self-consistent molecular orbital and band structure calculations (extended Hückel Hamiltonian). We will discuss the validity of a single-cluster approach to the electronic structures of the title compounds and investigate the possible influence of intercluster interactions. Such effects are important for the magnetic properties of α-Nb_3Cl_8 at low temperatures and become even more important for β-Nb_3Br_8 and β-Nb_3I_8.[7,8]

2. Experimental Section

2.1. Synthesis and Characterization. All starting materials and glassware were handled as previously described.[1] The procedure to form β′-$NaNb_3Cl_8$ followed a slightly modified method to that in the literature. All reactions were performed in a three-armed reaction vessel whereby the Na_2bzph−THF solution is prepared in one arm, this being

† Present Address: Idaho National Engineering Laboratory, Research Center, MS 2208, Idaho Falls, ID 83415.

⊗ Abstract published in *Advance ACS Abstracts,* March 15, 1996.

(1) Kennedy, J. R.; Simon, A. *Inorg. Chem.* **1991**, *30*, 2564.
(2) Mattausch, Hj.; Kennedy, J. R. Unpublished results.
(3) (a) Schöllhorn, R.; Steffen, R.; Wagner, K. *Angew. Chem.* **1983**, *95*, 559. (b) Steffen, R.; Schöllhorn, R. *Solid State Ionics* **1986**, *22*, 31.
(4) Schnering, H. G.; Wöhrle, H.; Schäfer, H. *Naturwissenschaften* **1961**, *6*, 159.
(5) Schnering, H. G.; Schäfer, H. *Angew. Chem.* **1964**, *76*, 833.
(6) (a) Cotton, F. A. *Inorg. Chem.* **1964**, *3*, 1217. (b) Bullet, D. W. *Ibid.* **1980**, *19*, 1780. (c) Bursten, B. E.; Cotton, F. A.; Hall, M. B.; Najjar, R. C. *Ibid.* **1982**, *21*, 302. (d) Müller, A.; Jostes, R.; Cotton, F. A. *Angew. Chem.* **1980**, *92*, 921.
(7) Simon, A.; von Schnering, H.-G. *J. Less-Common Met.* **1966**, *11*, 31.
(8) Niesert, B.; Dissertation, Universität Stuttgart, 1980.

0020-1669/96/1335-2276$12.00/0

decanted onto the solid α-Nb_3Cl_8 in the second (central) arm and filtered through the third arm.

In a drybox, a slight excess (relative to the α-Nb_3Cl_8 amount) of benzophenone is charged with a greater than 2-fold excess of fresh-cut sodium to the first vessel sidearm. Into the second (central) arm is added the α-Nb_3Cl_8 host compound (up to 10 g). The third arm contains a sintered glass-fritted filter attached to a Schlenk receiving flask. The reaction vessel is capped and removed from the box and THF either distilled or syringed onto the Na/bzph. This is allowed to stir for 20−30 h. The deep red-violet solution is then carefully decanted onto the α-Nb_3Cl_8 and allowed to react for approximately 10 h. The solution can be back-decanted onto the excess sodium in the first arm and the procedure repeated to ensure full intercalation. Finally, the entire mixture is filtered from the second arm through the third arm, washed several times with fresh THF, and dried in vacuum.

The powder X-ray diffractogram shows only lines belonging to β′-$NaNb_3Cl_8$. A Rietveld refinement[9] results in a weighted profile residual of $R_{wp} = 0.109$. Magnetic susceptibility measurements indicate a trace of paramagnetic impurities amounting to approximately 0.5% in case of unreacted α-Nb_3Cl_8.

2.2. Optical Spectroscopy. Thoroughly ground samples of α-Nb_3Cl_8 (green) and β′-$NaNb_3Cl_8$ (red-violet) were sealed in a quartz glass sample holder and measured at room temperature with a Perkin-Elmer Lambda 9 double beam spectrometer by the diffuse reflectance technique. For this purpose, the spectrometer was equipped with a 60 mm integrating sphere attachment, internally coated with $BaSO_4$ which was used as reference.

2.3. Photoelectron Spectroscopy. XPS and UPS measurements were performed with a Leybold-Heraeus LHS-10 spectrometer using nonmonochromatized Mg Kα (1253.6 eV), He I (21.2 eV), and He II (40.8 eV) radiation. The base pressure of the spectrometer was better than 3×10^{-10} mbar. The experiments were performed on pellets pressed from α-Nb_3Cl_8 and β′-$NaNb_3Cl_8$ powders (10 mm diameter) which were occasionally scraped in vacuum in order to expose the underlying surfaces of the ground and pressed powder samples. The samples appeared to be stable under UHV conditions. Energy calibration of the spectrometer was performed by measuring the $4f_{7/2}$ spectrum of a freshly sputtered gold foil (binding energy BE = 84.00 eV) with Mg Kα and the Au Fermi level with He I radiation. There were no apparent charging effects. In spite of scraping the samples prior to the measurements, a certain amount of oxygen contamination was observed at the surface, most likely having been accumulated during the grinding process. The O 1s signals were broad and did not show any structure.

3. Electronic Structure Calculations

The electronic structures of α-Nb_3Cl_8 and β′-$NaNb_3Cl_8$ were studied with the help of semiempirical charge−self-consistent[10] molecular orbital and band structure calculations using a simplified one-electron Hamiltonian within extended Hückel theory.[11] The reason for using such a semiempirical method lies in the large unit cell sizes of α-Nb_3Cl_8 (22 atoms) and β′-$NaNb_3Cl_8$ (72 atoms), summing up to 118 and 378 atomic wave functions (minimal valence orbital basis set) and providing for a convenient comparison between the results from band structure and subsequent molecular cluster model calculations.

In the beginning of the band calculations, on-site H_{ii} values were approximated by numerical atomic Hartree−Fock energies[12] while Slater-type orbital exponents were based on numerical atomic wave functions[13] (Na) or on Slater orbitals that had been fitted to numerical Herman−Skillman functions[14] (Nb,Cl). Counterintuitive orbital mixing effects were suppressed by obtaining off-site Hamiltonian matrix elements by the weighted Wolfsberg−Helmholz formula.[15] During the iterative process towards self-consistency, electron correlation was corrected up to first order by varying the atomic Coulomb integrals as a function of atomic charge and electronic configuration. The charge iteration parameters of the quadratic power series were taken from the literature.[10,16]

All computations were carried out on a DECstation 5000/133 machine using a modified[17] EHMACC program.[18] The eigenvalue problem was solved in reciprocal space at 28 (α-Nb_3Cl_8) and 24 *k* points (β′-$NaNb_3Cl_8$) within the irreducible wedge of the Brillouin zone. After having reached self-consistency (22 and 15 cycles respectively), another averaging over both phases yielded a unique set of converged exchange integral parameters and Slater exponents that could also be used for the molecular model computations using the CACAO programs.[19] The exchange integrals for all computations reported here were set to the following (ζ orbital exponents in parentheses): Na 3s, −7.18 eV (0.832); Na 3p, −5.06 eV (0.611); Cl 3s, −24.49 eV (2.227); Cl 3p, −12.38 eV (1.916); Nb 5s, −8.27 eV (1.428); Nb 5p, −5.31 eV (1.035). For greater accuracy, the Nb 4d atomic wave function (average orbital energy: −9.55 eV) was approximated by a double-ζ function with exponents $\zeta_1 = 2.955$, and $\zeta_2 = 1.333$ and weighting coefficients $c_1 = 0.686$ and $c_2 = 0.462$.

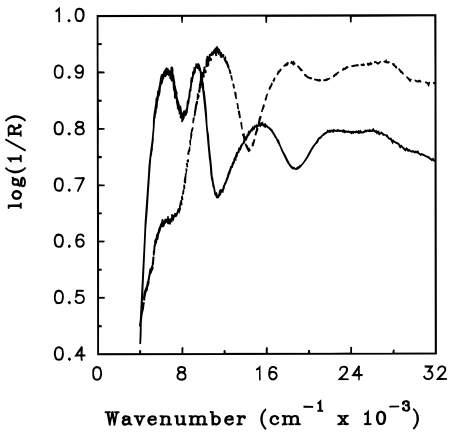

Figure 1. Logarithm of the inverse of the reflectance vs wave number for the compounds α-Nb_3Cl_8 (solid line) and β′-$NaNb_3Cl_8$ (dashed line).

Table 1. Optical Absorption Maxima for the Compounds (a) α-Nb_3Cl_8 and (b) β′-$NaNb_3Cl_8$

compound	wave number (cm^{-1})	wave length (nm)	energy (eV)
α-Nb_3Cl_8	6550	1527	0.81
	9450	1056	1.17
	15600	640	1.94
	22400	446	2.78
	26100	383	3.24
β′-$NaNb_3Cl_8$	6000	1670	0.74
	11290	890	1.40
	18250	548	2.26
	24300	412	3.01
	26900	372	3.34

4. Results

4.1. Optical Spectroscopy. The diffuse reflectance spectra for α-Nb_3Cl_8 and β′-$NaNb_3Cl_8$ over the range 4000−32000 cm^{-1} are illustrated in Figure 1 and the corresponding absorption maxima are tabulated in Table 1. The band widths are at least 2000 cm^{-1}. For α-Nb_3Cl_8, the absorptions with maxima at

(9) Kennedy, J. R. To be submitted for publication.
(10) McGlynn, S. P.; Vanquickenborne, L. G.; Kinoshita, M.; Carroll, D. G. *Introduction to Applied Quantum Chemistry*; Holt, Rinehart and Winston: New York, 1972.
(11) (a) Hoffmann, R. *J. Chem. Phys.* **1963**, *39*, 1397. (b) Hoffmann, R. *Solids and Surfaces: A Chemist's View of Bonding in Extended Structures*; VCH: Weinheim, Germany, New York, 1988.
(12) Desclaux, J. P. *At. Data Nucl. Data Tables* **1973**, *12*, 311.
(13) Pyykkö, P.; Lohr, L. L., Jr. *Inorg. Chem.* **1981**, *20*, 1950.
(14) Fitzpatrick, N. J.; Murphy, G. H. *Inorg. Chim. Acta* **1984**, *87*, 41; **1986**, *111*, 139.
(15) Ammeter, J. H.; Bürgi, H.-B.; Thibeault, J. C.; Hoffmann, R. *J. Am. Chem. Soc.* **1978**, *100*, 3686.
(16) Baranovskii, V. I.; Nikolskii, A. B. *Teor. Eksp. Khim.* **1967**, *3*, 527.
(17) Häussermann, U.; Nesper, R. ETH Zürich, unpublished.
(18) QCPE program EHMACC by Whangbo, M.-H.; Evain, M.; Hughbanks, T.; Kertesz, M.; Wijeyesekera, S.; Wilker, C.; Zheng, C.; Hoffmann, R.
(19) Program CACAO by Mealli, C.; Proserpio, D. M. *J. Chem. Educ.* **1990**, *67*, 399.

Table 2. XPS and UPS Binding Energies (eV) for α-Nb_3Cl_8 and β′-$NaNb_3Cl_8$

level	α-Nb_3Cl_8	β′-$NaNb_3Cl_8$
Nb $3d_{5/2}$	205.0(1)	204.8(1)
Cl $2p_{3/2}$	199.5(1)	199.8(1)
Na 1s		1072.8(1)
Nb 4d[a]	0.88, 1.92, 2.67	0.75, 1.20, 1.95, 2.45
Cl 3p[b]	6.5(3.9)	6.7(3.4)

[a] Peak maxima of the structures in the UP spectra. [b] Mean position of the XP valence band; full widths at half-maximum are given in parentheses.

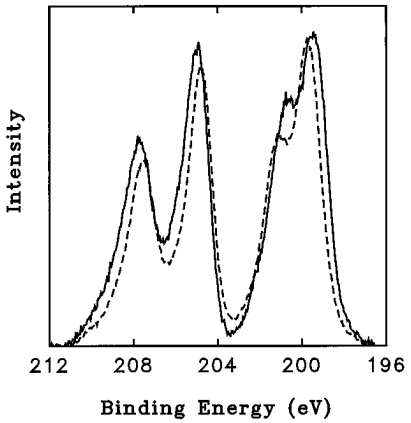

Figure 2. Nb 3d and Cl 2p core-level spectra for α-Nb_3Cl_8 (solid line) and β′-$NaNb_3Cl_8$ (dashed line).

15 600, 22 400, and 26 100 cm^{-1} are responsible for its green color and for β′-$NaNb_3Cl_8$, those with maxima at 11 290, 18 250, and 24 300 cm^{-1} for its red-violet color. At the low energy (near IR) side of the spectra, α-Nb_3Cl_8 shows two rather narrow absorptions at 6550 and 9450 cm^{-1} whereas β′-$NaNb_3Cl_8$ shows only a weak shoulder at about 6000 cm^{-1} and a broader absorption centered at 11 290 cm^{-1}.

4.2. Photoelectron Spectroscopy. The binding energies (BE) from the core level spectra are summarized in Table 2; the Nb 3d and Cl 2p spectra are depicted in Figure 2. The shapes of the spectral patterns for both compounds are very similar. The Nb 3d spectra show a single band for each of the $3d_{5/2}$ and $3d_{3/2}$ spin−orbit components. In addition, a broad plasmon band is found at higher binding energies (not shown in Figure 2). The BE for β′-$NaNb_3Cl_8$ is slightly smaller than that for α-Nb_3Cl_8. In comparison to α-Nb_3Cl_8, the Cl 2p bands for β′-$NaNb_3Cl_8$ occur at about 0.3 eV higher in binding energy. The resolution of the Cl 2p spectra (which consist of the $2p_{3/2}$ and $2p_{1/2}$ spin−orbit components) does not allow us to identify the four different bonding types of chlorine in the crystal structures of α-Nb_3Cl_8 and β′-$NaNb_3Cl_8$. The Cl 2p signal for β′-$NaNb_3Cl_8$, however, is slightly more narrow than that for α-Nb_3Cl_8. The binding energy for the Na 1s core level is rather high (*cf.* BE = 1071.4 eV for NaCl).

The valence band spectra of α-Nb_3Cl_8 and β′-$NaNb_3Cl_8$, measured with different excitation energies, are given in Figures 3 and 4. In order to guide the interpretation of the spectra, the atomic photoionization cross sections[20] for the relevant orbitals are summarized in Table 3. Also included are the O 2p cross sections since a not insignificant amount of oxygen contamination was found at the surface as judged from the XP spectra. From these data and sample composition, it is evident that the Mg Kα and the He I spectra should be dominated by photoemission from Cl 3p orbitals whereas the He II spectrum should be dominated by photoemission from Nb 4d orbitals. The

(20) Yeh, J. J.; Lindau, I. *At. Data Nucl. Data Tables* **1985**, *32*, 1.

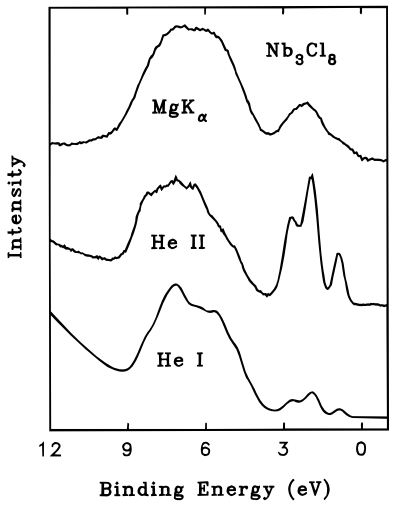

Figure 3. Valence band spectra of α-Nb_3Cl_8 for different excitation sources.

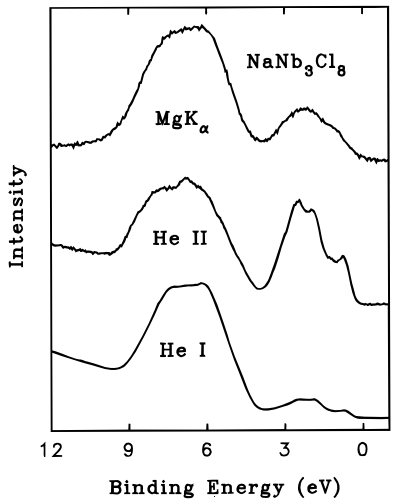

Figure 4. Valence band spectra of β′-$NaNb_3Cl_8$ for different excitation sources.

Table 3. Theoretical atomic Photoionization Cross Sections According to Yeh and Lindau[20]

level	He I: 21.2 eV	He II: 40.8 eV	Mg Kα: 1253.6 eV
Nb 4d	22.10	4.66	0.46×10^{-2}
Cl 3p	13.84	0.65	0.33×10^{-2}
O 2p	10.67	6.82	0.5×10^{-3}

experimental valence band spectra of both α-Nb_3Cl_8 and β′-$NaNb_3Cl_8$ consist of two groups of bands. Whereas the intensities of the bands at higher binding energies are strong in the Mg Kα and He I spectra, the intensity contributions of the low binding energy bands are most pronounced in the He II spectra. Consequently, the electronic structure of these niobium chlorides is characterized by sets of well-separated Cl 3p and Nb 4d orbitals. The Cl 3p orbitals are lower in energy and give rise to the high binding energy part of the valence band spectra whereas the Nb 4d orbitals determine the highest occupied states which occur at lower binding energies. The Nb 4d part of the UP spectra of α-Nb_3Cl_8 is well resolved and reveals a three-peak structure (BE 0.88, 1.92, and 2.67 eV).

The XP valence band spectrum of β′-$NaNb_3Cl_8$ shows an increased photoemission intensity at the lowest binding energies compared to that of α-Nb_3Cl_8. The better resolved UP spectra reveal a more complicated structure for the Nb 4d derived levels. In agreement with the Cl 2p core level spectra, the Cl 3p valence band spectra of β′-$NaNb_3Cl_8$ are sharper than those for α-Nb_3-

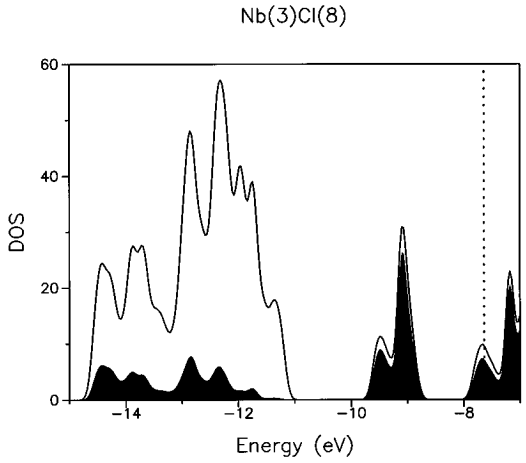

Figure 5. Density-of-states (DOS) for α-Nb_3Cl_8. The Nb contribution is emphasized in black; the Fermi level is given as a dotted line.

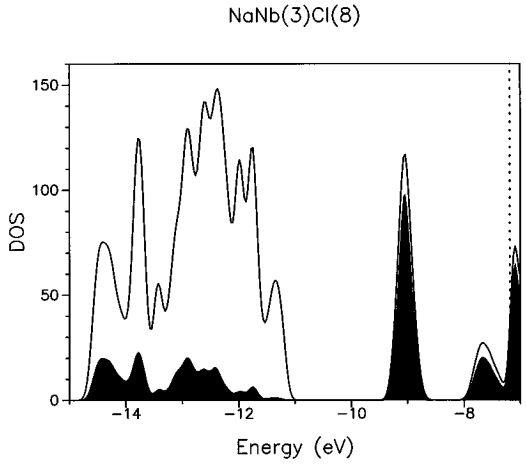

Figure 6. DOS for β′-$NaNb_3Cl_8$.

Cl_8. Finally, the Cl 3p region of the UP valence band spectra is presumably disturbed by surface oxygen 2p contributions which should have the strongest effect in the He II spectra (Table 3). The contaminations are expected to give rise to a broad structureless band (the O 1s band is also observed to be broad), superimposed on the Cl 3p photoemission. The rather sharp structures seen in the UP spectra, especially for α-Nb_3Cl_8, are probably intrinsic. The XP valence band spectra are not disturbed by photoemission from O 2p orbitals.

4.3. Band Structure Calculations. The results of the band structure calculations are illustrated in Figures 5 and 6, depicted as partial and total density-of-states (DOS) curves for α-Nb_3Cl_8 and β′-$NaNb_3Cl_8$, both within an energy range of −15 to −7 eV. The contribution of the Nb atoms is emphasized in black. For both compounds one observes a clear separation between the levels at higher energy (above −10 eV) and those at lower energy, which have primarily niobium and chlorine character respectively.

5. Discussion

5.1. Crystal Structure, Electronic Structure, and Valence Band Spectra. The basic structure of the $Nb_3Cl_8^{n-}$ ($n = 0, 1$) compounds is common to a variety of compounds including the bromide and iodide analogues as well as a number of molybdenum oxide counterparts $Mo_3O_8^{n-}$ ($n = 4, 5, 6$).[7,21,22] The compounds form as layered structures where M_3X_8 represents one X−M−X layer and the ultimate structure is determined from the relative orientations of the layers. Each M_3X_8 layer can be imagined as being built from M_3X_{13} clusters whereby nine of the 13 X atoms are shared between one or more adjacent lying M_3X_4 units in the trigonal cell according to $M_3X_{13} = M_3(X^1)_{6/2}(X^2)_{3/1}(X^3)_{3/3}(X^4)_{1/1} = M_3X_8$.[23] Thus, the central M_3X_4 unit is built from one X^4 atom face bridging the M_3 triangle on one side with three X^2 centers edge bridging each of the edges of the triangle on the opposing side. The intercluster bridging X^1 and X^3 atoms are terminal ligands in M_3X_{13} but bridge between two or three neighboring clusters respectively in M_3X_8. The X^1 site is found on the same side of the triangle as X^4, and X^3 is on the X^2 side. An illustration of the structure is provided in Figure 7. The electron-donating Na cations lie in octahedral sites between the layers.[9]

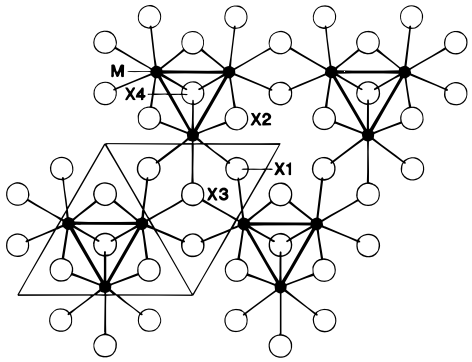

Figure 7. Illustration of a layer of the M_3X_8 structure.

Since the M_3X_8 structure can be thought to form from interconnecting M_3X_{13} clusters, one can get an idea of the electronic structure of the M_3X_8 compounds by first considering the molecular orbital diagram of an M_3X_{13} cluster.[6] Here, assigning the metal (in this case niobium) one 5s, three 5p, and two 4d atomic orbitals to interact with the six chloride ligands in the octahedral field about each metal atom center, then three d atomic orbitals on each metal atom center (or a total of nine d orbitals for the M_3 triangle) remain for metal−metal interactions within the cluster. Under the strict C_{3v} local symmetry of the M_3X_{13} cluster in the M_3X_8 structure, these nine atomic orbitals transform to four bonding and five antibonding combinations. The four bonding molecular orbitals reduce as $1a_1 < 1e < 2a_1$.

These molecular orbitals, as obtained from a model calculation on a perfectly C_{3v} symmetric molecular $Nb_3Cl_{13}^{5-}$ anion (coordinates taken from the α-Nb_3Cl_8 crystal structure) are illustrated pictorially in Figure 8, and the energy level diagram of the metal-centered orbitals is depicted in Figure 9. The most strongly metal−metal bonding MO is the lowest lying (−9.47 eV) $1a_1$ level (Figure 8a) which can be described as being composed of three d_{z^2} Nb wave functions (with respect to a local atomic coordinate system) pointing into the middle of the Nb triangle. While the main electron density for this particular MO is indeed located in the very center of the Nb triangle, a similar directional tendency is less pronounced for the degenerate 1e levels at −8.95 eV (Figure 8b). The weakly bonding $2a_1$ MO (−7.67 eV), on the other hand, leads to Nb−Nb bonding a little outside of the edges of the Nb triangle (Figure 8c).

In the case of α-Nb_3Cl_8, there are $(3 \times 5) - (8 \times 1) = 7$ electrons available to occupy these bonding orbitals which results in a half filled $2a_1$ HOMO (Figure 9) yielding a $^2A_1$ ground state. For β′-$NaNb_3Cl_8$, having one additional electron, the $2a_1$ HOMO is fully occupied to give a $^1A_1$ ground state.

(21) Torardi, C. C.; McCarley, R. E. *Inorg. Chem.* **1985**, *24*, 476.
(22) Ansell, G. B.; Katz, L. *Acta Crystallogr.* **1966**, *21*, 482.
(23) Atom-numbering scheme according to ref 21.

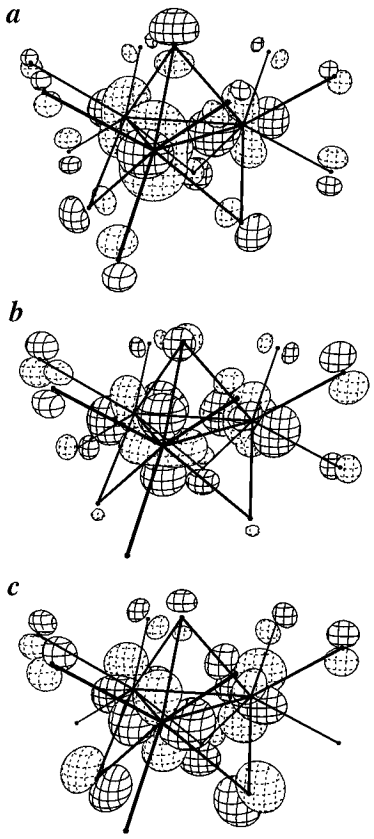

Figure 8. Nb-centered molecular orbitals of an $Nb_3Cl_{13}^{5-}$ molecular anion in point group C_{3v}. Depicted are the (a) $1a_1$ (−9.47 eV), (b) 1e (−8.95 eV), and (c) $2a_1$ (−7.67 eV) molecular orbitals.

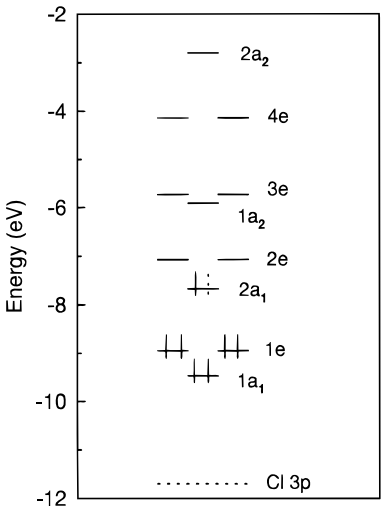

Figure 9. Energy level diagram of the Nb-centered molecular orbitals for an $Nb_3Cl_{13}^{n-}$ unit in point group C_{3v}. The $2a_1$ HOMO is singly occupied for a seven electron cluster ($n = 5$) and doubly occupied for an eight electron cluster ($n = 6$). The highest energy chlorine states are indicated by a dashed line.

Thus, α-Nb_3Cl_8 exhibits Curie−Weiss paramagnetism[7] whereas β'-$NaNb_3Cl_8$ shows a weak temperature independent paramagnetism.[1,9]

This simple, with respect to Nb−Cl bonding, mainly ionic model is well supported by the X-ray and UV valence band photoelectron spectra of α-Nb_3Cl_8 (Figure 3). As described above, the spectra consist of a broad, somewhat structured band with mainly chlorine 3p character lying at higher binding energies to a band of mainly niobium 4d character which, in the He I and He II spectra, resolves into a triple-peak structure. The energy separation between the chlorine 3p and niobium 4d bands is about one electron volt. The shapes of the niobium bands reflect the positioning of the $1a_1$, 1e, and $2a_1$ metal−metal bonding MO's. The relative intensities of the three peaks in the UP spectra are consistent with the orbital occupancies 2:4:1 expected for a seven electron Nb_3 cluster.

A similar triple-peak structure is also seen in the theoretical density-of-states curve (Figure 5) obtained from the charge-self-consistent extended Hückel calculation for the real solid. The relative energy differences between the $1a_1$, 1e, and $2a_1$ levels obtained from the experimental binding energies ($1a_1$−1e = 0.75 eV, 1e−$2a_1$ = 1.04 eV) compare well with those from the band structure calculation (0.40 and 1.41 eV respectively). The energy difference between the $1a_1$ and $2a_1$ levels is practically the same in both the experimental data (1.79 eV) and theoretical description (1.82 eV). Referring to the partial density-of-states in Figure 5, it is also clear that there is a well reproduced energy separation (1.2 eV) between lower lying primarily chlorine states and higher lying niobium states. The relative intensities of the upper levels in the calculated densities of states is also fully satisfactory when one takes into account that the Fermi level is positioned in the middle of the DOS peak corresponding to the half-filled molecular $2a_1$ level. Since its intensity must therefore be taken as one half of that illustrated in Figure 5, the relative intensities of the extended Hückel DOS also correspond to 2:4:1.

The Fermi level is found in the middle of the DOS peak; however, this is not in contradiction with conductivity measurements[24] and the photoelectron spectra which reveal a significant band gap at room temperature. Since the highest band is practically without dispersion, the unpaired electron is physically trapped on the individual cluster due to vanishing intercluster hopping. Such truly local electronic shielding effects are typically not reproduced by any band theory.

Recently, a semiempirical band structure calculation on the bromine analogue β-Nb_3Br_8 has been published.[25] Similar to the present results on α-Nb_3Cl_8, well-separated sets of Br 4p and Nb 4d levels were obtained, the latter also revealing a triple-peak structure. However, the calculated energy gap between the highest Br 4p and lowest Nb 4d levels was more than 2 eV, which is considerably larger than the Cl 3p/Nb 4d separation of roughly 1 eV obtained both experimentally and theoretically for α-Nb_3Cl_8. This is in disagreement with the usual trend for charge transfer energies in transition metal halides[26,27] which decrease in going from the fluorides to the iodides. Also, the dark, almost black color of β-Nb_3Br_8 is in favor of a smaller charge transfer energy. On closer inspection, the reason of this discrepancy can be traced back to the choice of parameters in that specific calculation on β-Nb_3Br_8.

The overall ionic picture concerning Nb−Cl bonding is retained in the sodium intercalated phase β'-$NaNb_3Cl_8$. This is again seen from the dependence of the relative intensities of the valence band spectra on the energy of the excitation radiation (Figure 4). Comparing first the XP spectra of α-Nb_3Cl_8 and β'-$NaNb_3Cl_8$, where disturbances due to surface oxygen 2p emission are negligible, we observe for β'-$NaNb_3Cl_8$ a narrowing of the chlorine 3p band and a gain in relative intensity of the niobium 4d band. For a more quantitative analysis, the XP valence band spectra were background-corrected and integrated to give the chlorine 3p/niobium 4d area ratios.[28] The intensity

(24) Kepert, D. L., Marshall, R. E. *J. Less-Common Met.* **1974**, *34*, 153.
(25) Meyer, H.-J. *Z. Anorg. Allg. Chem.* **1994**, *620*, 81.
(26) Lever, A. B. P. *Inorganic Electronic Spectroscopy*; Elsevier: Amsterdam, Oxford, New York, Tokyo, 1984.
(27) Zaanen, J.; Sawatzky, G. A. *J. Solid State Chem.* **1990**, *88*, 8.
(28) In order to obtain the relative Cl 3p and Nb 4d weights, both bands were each fitted to three Gaussian profiles.

ratios (I_{3p}/I_{4d}) are 4.4 for α-Nb_3Cl_8 and 3.7 for β′-$NaNb_3Cl_8$. According to the cluster model, the ratios of these two numbers should equal 8/7 ≈ 1.14 which compares well with the experimental value of 1.19.

On the basis of this analysis, one expects a triple-peak structure with an intensity ratio of 1:2:1 for the niobium derived states of β′-$NaNb_3Cl_8$. The better resolved He I and He II spectra, however, reveal a more complicated structure. In comparison to α-Nb_3Cl_8, the Nb 4d part of the spectra is broadened with an unexpected high density-of-states occurring in the high binding energy part, which suggests a certain stabilization of some of the low energy metal−metal bonding 4d levels. This structure can not be understood within the molecular model. In contrast to the behavior of the Nb 4d levels, the Cl 3p part of the spectra becomes more narrow with the highest occupied Cl 3p levels of β′-$NaNb_3Cl_8$ occurring at higher binding energies than those of α-Nb_3Cl_8.

Considering these experimental findings, one may ask whether intercluster interactions leading to a stronger splitting of the Nb 4d states in the solid are more important for β′-$NaNb_3Cl_8$ than for α-Nb_3Cl_8. Similar to that of α-Nb_3Cl_8, the calculated DOS for β′-$NaNb_3Cl_8$ (Figure 6) also shows a broad, fairly well structured band of primarily chloride states lying at lower energy to the higher occupied orbitals of mostly niobium character. In contrast to α-Nb_3Cl_8, however, only two niobium-centered bands appear with relative intensities of about 3:1. This is not expected from the simple rigid band model described at the beginning of the discussion whereby one electron would be simply added to fill the highest lying $2a_1$ orbital. On closer analysis, it appears that whereas the two highest lying orbitals have not changed their energies to any significant amount, the lowest lying band that corresponds to the molecular $1a_1$ level has increased its energy and effectively run into the 1e band. The reason for this destabilization can be understood by referring to Figure 8a, where the character of this $1a_1$ molecular orbital is pictorially illustrated. Besides the aforementioned contributions of niobium d wave functions pointing inside the Nb triangle, there is an antiphase mixing in of the X^4 face-bridging chloride p orbital. According to the crystallographic data,[9] the distance between the Nb triangle plane and this X^4 chlorine atom is shorter (about 10 pm) in β′-$NaNb_3Cl_8$ than in α-Nb_3Cl_8. Consequently, the anti-phase interaction closes the $1a_1-1e$ energy gap by pushing the $1a_1$ level up by more than 40% in a model calculation on the corresponding molecular $Na_4Nb_3Cl_{13}^{2-}$ anionic unit of the crystal structure. A more systematic series of calculations in which the niobium triangle−chlorine distance was varied (neglecting changes in the electron count), revealed a monotonic decrease in the $1a_1-1e$ energy gap as this specific distance was decreased. The total effect over the entire bonding within the cluster is a strengthening of the Nb−Cl bonding and a less pronounced weakening of the Nb−Nb bonding. This local effect is only weakly enhanced by the additional (second-nearest neighbor) coupling between the clusters in the solid.

From the theoretical DOS curve, one should expect a narrowing of the Nb 4d part of the valence band spectra in β′-$NaNb_3Cl_8$, just the opposite of the experimental observation. To resolve this discrepancy, one may first consider a breakdown of the effective one-electron theory, giving in the case of β′-$NaNb_3Cl_8$ a false representation of the density-of-states around −9 eV due to inadequate treatment of electron correlation. However, one has to reconsider that there is a rather close (almost quantitative) correspondence between the valence band photoelectron spectra and the theoretical DOS curves for α-Nb_3Cl_8, an "open-shell" system where electron correlation could be expected to play a major role. Thus, there is no physical argument at hand that would call for a failure of the theoretical method in the β′-$NaNb_3Cl_8$ "closed-shell" system which should present less difficulties. In other words, it is very unlikely that this discrepancy between experiment and theory is due to a breakdown of the electron theory used here.

Accordingly, one may question whether the photoelectron spectra of β′-$NaNb_3Cl_8$ do really represent the bulk electronic structure and whether peculiarities due to the nature of the photoemission experiment are present. The latter may arise either from final state effects or from surface related effects.

Concerning final state effects, the following is considered. Since for the "open shell" system α-Nb_3Cl_8, both singlet as well as triplet final states are possible and for β′-$NaNb_3Cl_8$ only doublet final states should occur, there is no reason why the valence band spectra of β′-$NaNb_3Cl_8$ should be more complicated than those of α-Nb_3Cl_8.

Concerning the second possibility, one may suspect that the presence of oxygen at the surface of the measured samples could result in chemically different types of clusters. However, the oxygen peaks in all samples were observed to be broad and gave no indication of Nb−O bond formation. In addition, that there were very little differences between the O 1s peaks in the α-Nb_3Cl_8 and β′-$NaNb_3Cl_8$ spectra is not consistent with the observation of a triple-peak structure in the valence band spectra of the former and a more complicated one in those of the latter. Also, the Nb 3d and Cl 2p core level peaks are more narrow for β′-$NaNb_3Cl_8$ than for α-Nb_3Cl_8, which does not correspond to the drastic differences expected in these signals from such chemically modified species.

Another possibility for a surface effect arises from the presence of sodium cations between the Nb_3Cl_8 layers of β′-$NaNb_3Cl_8$, an argument that is related to the composition of the surface. In the case of α-Nb_3Cl_8, the composition of the surface layer is certainly the same as for any bulk layer. In bulk β′-$NaNb_3Cl_8$, any electron donating sodium cation is surrounded by cluster layers on both sides of it. The surface sodium cations, on the other hand, can donate their electrons only to one layer, the surface layer. Therefore, one might expect a different sodium content at the surface or, alternatively, clusters with different electron numbers in order to maintain the charge balance. The broadening of both the XP and UP valence band spectra (differing in their surface sensitivity) indicates that such effects are probably not restricted to the first surface layer but do rather appear in a more extended depth between surface and bulk. Unfortunately, a detailed analysis of the XP spectrum is prevented by its lower resolution. As a consequence, a *distribution* of energy levels may give rise to the broad Nb 4d valence band structure. On the other hand, the more narrow Nb 3d, Cl 2p, and Cl 3p bands for β′-$NaNb_3Cl_8$ do not favorably support such a surface effect.

In conclusion, whereas the overall agreement between chemical bonding models and valence band spectra is excellent for α-Nb_3Cl_8, the detailed valence band shape for β′-$NaNb_3Cl_8$ is hard to interpret and still awaits an ultimate explanation. Other experiments directed at mapping the occupied and unoccupied density of states with less surface sensitive techniques would be helpful to resolve this problem.

5.2. Core Level Spectra. A study on a series of niobium iodide compounds revealed a linear relationship between the binding energy of the Nb $3d_{5/2}$ spin−orbit component and the formal oxidation state derived from the Nb/I ratio.[29] The two compounds studied here are in agreement with this general trend whereby the BE of the Nb $3d_{5/2}$ component of the reduced

(29) Geyer-Lippmann, J.; Simon, A.; Stollmaier, F. *Z. Anorg. Allg. Chem.* **1984**, *516*, 55.

species β'-$NaNb_3Cl_8$ is found at about 0.1−0.2 eV lower than that of α-Nb_3Cl_8. This difference is, however, at the error limit. The Nb $3d_{5/2}$ BE value of α-Nb_3Cl_8 is about 0.3 eV higher than that reported for the iodide analogue β-Nb_3I_8 (204.7 eV). This is probably due to a less positive charge on the Nb atoms in β-Nb_3I_8 as a consequence of the increased covalency of the Nb−I bonds compared with the more ionic Nb−Cl bonds.

The Cl 2p bands (Figure 2) for both α-Nb_3Cl_8 and β'-$NaNb_3Cl_8$ lie at energies consistent with the bridging character of their bonding. The Cl 2p spectrum of the intercalated phase is shifted by about 0.3 eV to higher BE and is slightly narrower. These observations are attributed to a stronger bonding of the six doubly bridging Cl^1 and Cl^2 atoms through electrostatic interactions with the sodium cations. The triply bridging Cl^3 and Cl^4 atoms, which are expected to occur at slightly higher BE than the doubly bridging Cl atoms, are much more separated from the sodium cations and thus less affected by electrostatic interactions. The greater stabilization of the Cl^1 and Cl^2 atoms relative to the Cl^3 and Cl^4 atoms will effectively push the former bands into the latter, resulting in an overall narrowing of the Cl 2p spectrum. These electrostatic interactions are also at least partly responsible for the differences in the Cl 3p valence band spectra.

5.3. Optical Spectra. The optical spectra provide some information about the unoccupied states which are lowest in energy. The two rather narrow absorption peaks at 6550 and 9450 cm^{-1} (0.81 and 1.17 eV respectively) for α-Nb_3Cl_8 can be assigned to the $1e-2a_1$ ($^2A_1-^2E$) and $1a_1-2a_1$ ($^2A_1-^2A_1$) transitions, this is from the lower lying Nb−Nb bonding MO's into the singly occupied highest MO. The corresponding energies derived from the EH band structure calculation are 1.41 and 1.82 eV; those from the photoelectron spectra are 1.04 and 1.79 eV. Any comparison between ground state band structure (or molecular orbital) calculations and photoemission experiments on the one side and optical spectra on the other should be taken with prudence because the optical transitions involve changes in Coulomb repulsion energy. In addition, the equilibrium spatial coordinates may be different in the excited state. These two transitions are not possible in β'-$NaNb_3Cl_8$ because the $2a_1$ orbital is fully occupied and thus the corresponding absorptions are absent (Figure 1b).

Molecular orbital theory suggests the lowest unoccupied orbital to be the 2e orbital. Accordingly, a $2a_1-2e$ ($^1A_1-^1E$) transition would be the lowest energy spin-allowed excitation. For β'-$NaNb_3Cl_8$, this presumably corresponds to the broad absorption band centered at 11 290 cm^{-1} (1.40 eV). The shoulder at about 6000 cm^{-1} (0.74 eV) may arise from either a small amount of impurity α-Nb_3Cl_8 phase or correspond to the spin-forbidden $^1A_1-^3E$ transition.[30] The $2a_1-2e$ ($^2A_1-^2E$) transition should also exist for α-Nb_3Cl_8 and is tentatively attributed to the 1.93 eV band. Optical studies on single crystals are required for a more detailed discussion of the excited states.

6. Conclusions

We have studied the electronic structures of the compounds α-Nb_3Cl_8 and β'-$NaNb_3Cl_8$ experimentally and theoretically by X-ray and UV photoelectron spectroscopy, optical spectroscopy, and charge-self-consistent band structure and molecular orbital calculations. The overall electronic structure for both α-Nb_3Cl_8 and β'-$NaNb_3Cl_8$ is characterized by sets of separated Cl 3p and Nb 4d orbitals which evidences that the degree of ionic Nb−Cl interactions is significant, as expected. In this respect, the electronic structures of the present niobium chlorides are similar to those of the zirconium chlorides $ZrCl_x$ ($x = 1-3$).[31] The experimental valence band spectra of α-Nb_3Cl_8 agree well with the theoretical DOS curve which essentially corresponds to the molecular orbitals of a seven electron Nb_3 cluster. Also, the low energy excitations in the optical spectrum of α-Nb_3Cl_8 can be qualitatively understood within a single cluster model. The XP valence band spectra of β'-$NaNb_3Cl_8$ evidence an additional electron in the Nb 4d levels as expected from electron counting rules. The detailed structure of the UP valence band spectra, however, is more complicated and is in disagreement with both the extended band structure and the molecular orbital model calculations. We have discussed the possibility that this discrepancy may be related to a surface composition differing from the bulk. The true origin of the disagreement between experiment and theory remains to be clarified.

Acknowledgment. We would like to thank Willi Hölle for carefully performing the photoemission experiments and Alf Breitschwerdt for measuring the diffuse reflectance spectra.

IC951348B

(30) Diffuse reflectance spectra are damped in comparison to transmission spectra and also weak absorptions may appear rather strong, see: Kortüm, G. *Reflexionsspektroskopie*; Springer: Berlin, Heidelberg, Germany, New York, 1969.

(31) Corbett, J. D.; Anderegg, J. W. *Inorg. Chem.* **1980**, *19*, 3822.